Molecular Cell, Vol. 16, 59–68, October 8, 2004, Copyright ©2004 by Cell Press

Drp-1-Dependent Division of the Mitochondrial Network Blocks Intraorganellar Ca^{2+} Waves and Protects against Ca^{2+}-Mediated Apoptosis

György Szabadkai,[1,3] Anna Maria Simoni,[1,3] Mounia Chami,[1] Mariusz R. Wieckowski,[1] Richard J. Youle,[2] and Rosario Rizzuto[1,*]

[1]Department of Experimental and Diagnostic Medicine
Section of General Pathology and
Interdisciplinary Center for the Study of Inflammation
University of Ferrara
44100 Ferrara
Italy

[2]Biochemistry Section
Surgical Neurology Branch
National Institute of Neurological Disorders and Stroke
National Institutes of Health
Bethesda, Maryland 20892

Summary

By transiently or stably overexpressing the mitochondrial fission factor dynamin-related protein-1 (Drp-1), we evaluated the role of mitochondrial division in organelle Ca^{2+} homeostasis and apoptotic signaling. Quantitative 3D digital microscopy revealed a split mitochondrial network in Drp-1-overexpressing cells without changes in cell viability. High-speed mitochondrial $[Ca^{2+}]$ ($[Ca^{2+}]_m$) imaging revealed propagating intramitochondrial Ca^{2+} waves in intact cells, which were blocked in the Drp-1-fragmented network, leaving a fraction of individual mitochondria without substantial $[Ca^{2+}]_m$ elevation. Consequently, in Drp-1-expressing cells the apoptotic efficacy of ceramide, which causes a Ca^{2+}-dependent perturbation of mitochondrial structure and function, was drastically reduced. Conversely, the sensitivity to staurosporine-induced apoptosis, previously shown to be directly triggered by Drp-1-dependent recruitment of proapoptotic proteins to mitochondria, was enhanced. These results demonstrate that the regulated process of mitochondrial fusion and fission controls the spatiotemporal properties of mitochondrial Ca^{2+} responses and, thus, physiological and pathological consequences of cellular Ca^{2+} signals.

Introduction

Two important means have been recently characterized that might adapt mitochondrial function to various conditions of the living cell: dynamic structural changes of the mitochondrial network, including continuous remodeling by fusion and fission events, and regulation of mitochondrial $[Ca^{2+}]$ ($[Ca^{2+}]_m$). Two groups of proteins involved in mitochondrial fusion and fission have been described comprising dynamin-like large GTPases and anchoring proteins of the outer mitochondrial membrane (OMM) (Yoon and McNiven, 2001; Mozdy and Shaw, 2003). However, little is known about the consequences of these frequently occurring dynamic structural changes. The evolutionarily highly conserved process of mitochondrial division is fundamental during cell division and, together with organelle biogenesis, was proposed to match the increased energy demand during cell differentiation and in response to toxin exposure (Yaffe, 1999). On the other hand, mitochondrial fission occurs during pathophysiological events, such as neurodegeneration, cellular aging, and apoptosis (Karbowski and Youle, 2003). Accordingly, the large GTPase dynamin-related protein-1 (Drp-1), driving the mitochondrial fission machinery, was shown to be associated with proapoptotic members of the Bcl-2 family proteins at mitochondrial scission sites during the apoptotic process (Frank et al., 2001; Breckenridge et al., 2003); however, neither the Drp-1 protein per se nor mitochondrial scission by itself has been shown to induce cell death.

Intramitochondrial Ca^{2+} seems to play a similar two-faced role in the regulation of mitochondrial function. Mitochondria take up Ca^{2+} avidly from the cytoplasm during agonist-induced Ca^{2+} signals, due to the strong driving force ensured by the membrane potential via a channel (Ca^{2+} uniporter, MCU) that was recently shown to be highly selective for Ca^{2+} and to require high external $[Ca^{2+}]$ for its opening (Kirichok et al., 2004). Indeed, efficient mitochondrial Ca^{2+} uptake in intact cells was shown to be dependent on the close apposition of mitochondria to Ca^{2+} release (endoplasmic reticulum, ER) and entry sites (plasmamembrane) where microdomains with high $[Ca^{2+}]$ are formed (Rizzuto et al., 1998; Csordas et al., 1999). Ca^{2+}-dependent stimulation of NAD(P)H and consequent ATP production, through activation of Ca^{2+} sensitive dehydrogenases and metabolite carriers, serves to adapt energy and substrate production to increased cellular needs (McCormack et al., 1990). In addition, mitochondria also serve as an intracellular Ca^{2+} buffer shaping cellular Ca^{2+} signals (Duchen, 2000). Mitochondrial Ca^{2+} loading, originating from Ca^{2+} release from the ER, has also been shown to play a crucial role in apoptosis induction caused by certain proapoptotic stimuli, such as C_2 ceramide (Szalai et al., 1999; Pinton et al., 2001). C_2 ceramide was shown to directly induce Ca^{2+} release from the ER Ca^{2+} store (Pinton et al., 2001) and also to sensitize mitochondria to Ca^{2+} impulses from $InsP_3$ or ryanodine receptor ($InsP_3R$, RyR)-mediated Ca^{2+} release, leading to mitochondrial permeability transition (MPT) and depolarization. This is followed by the release of proapoptotic factors activating the effector caspases and, finally, triggering apoptotic cell death (Orrenius et al., 2003). Importantly, mitochondrial depolarization in these cases is propagated as a wave throughout the cells, pointing to a fundamental role of mitochondrial network integrity in apoptotic signaling (Pacher and Hajnoczky, 2001).

Here we combine morphological and dynamic Ca^{2+} imaging to investigate the effect of forced mitochondrial division on intramitochondrial Ca^{2+} dynamics with cell population measurements to assess overall changes of mitochondrial Ca^{2+} and apoptotic signaling. Our results show that (1) the morphology of the mitochondrial net-

*Correspondence: r.rizzuto@unife.it
[3]These authors contributed equally to this work.

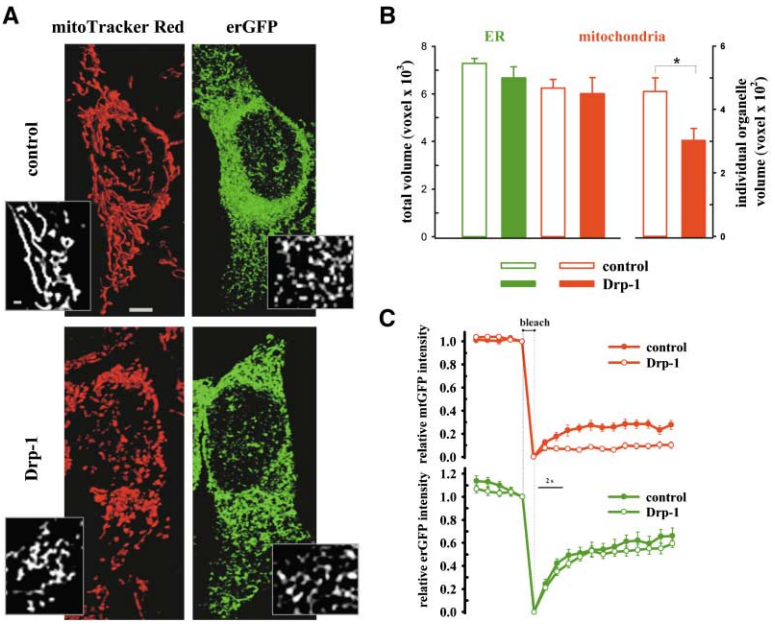

Figure 1. Morphological Analysis of the ER and Mitochondrial Networks in Drp-1-Expressing Cells

HeLa cells were transiently transfected with erGFP (control, open bars) or erGFP and Drp-1 (Drp-1-overexpressing cells, filled bars) and loaded with MitoTracker Red (see Experimental Procedures). Images acquired by digital microscopy were deconvolved, 3D reconstructed, and quantitatively analyzed. (A) Representative 3D reconstructed images of control (upper panels) and Drp-1-overexpressing cells (lower panels) showing Drp-1 induced fragmentation of the mitochondrial network and preserved ER structure. Insets (greyscale) show a selected focal plane from the 3D projection images. Scale bars indicate 10 μm (3D images) and 2 μm (insets). (B) Effect of Drp-1 overexpression on total organelle volume (left; green bars: ER, red bars: mitochondria) and individual particles of mitochondria (right). Data were obtained from 12 cells examined from three separate experiments (asterisk, $p < 0.001$). (C) Fluorescence recovery after photobleaching (FRAP) analysis of the mitochondrial (upper panel) and the ER network (lower panel) continuity. Bleaching of GFP fluorescence was applied in an approximately 10 μm circle at randomly chosen regions where indicated (bleach), and fluorescence intensity was normalized to the intensity levels before and after bleaching. Data were obtained from 18 cells examined from three separate experiments.

work and its contacts with the ER determine the spatial and quantitative nature of the mitochondrial Ca^{2+} signal, and (2) the mitochondrial network integrity and division play an important role in cellular resistance and sensitivity to apoptosis.

Results

Morphological Changes of the Mitochondrial Network in Drp-1-Overexpressing Cells

In order to evaluate the role of Drp-1 in determining mitochondrial morphology and its relationship with the ER, we used transient and stable/inducible overexpression models of the protein. In the transient expression model, quantitative morphological imaging of the mitochondrial and ER networks was applied to HeLa cells transfected with ER-targeted GFP (erGFP, controls), or erGFP cotransfected with Drp-1, to visualize the ER. In order to simultaneously reveal mitochondrial structure, the cells were loaded with MitoTracker Red. After deconvolution and 3D reconstruction (Figure 1A), the images were analyzed, evaluating two main aspects, overall volume and size distribution of individual mitochondrial/ER objects. Figure 1B shows that overexpression of Drp-1 did not affect either the mitochondrial or the ER total volume but caused fragmentation of the mitochondrial network, confirmed by the significant reduction of the average individual particle size of mitochondria. Conversely, the ER was represented by one large continuous compartment, as previously reported by Petersen and coworkers (Petersen et al., 2001), and no difference in organelle continuity was detected between Drp-1-overexpressing and control cells (an extensive, continuous object contained 91% ± 6% versus 89% ± 8% of the total ER volume, respectively). The fragmentation was thus specific for the mitochondrial network. Similar changes were observed in the inducible T-Rex-Drp-1 HeLa cell clone after 48 hr of induction (see below) or when a mitochondrially targeted GFP chimera was employed for labeling the organelle (data not shown). In order to evaluate the functional connectivity of the mitochondrial and ER networks, we carried out experiments with the fluorescence recovery after photobleaching (FRAP) technique in HeLa cells transiently expressing mtGFP (controls) or erGFP (Drp-1 cotransfected cells). As shown in Figure 1C, after bleaching randomly chosen regions in the Drp-1-fragmented mitochondrial network, we detected a fast but minor (9.20% ± 2.5%, at 10 s) refilling demonstrating that diffusion of mtGFP in the mitochondrial matrix occurred only from a small distance in the nonbleached region. In contrast, mitochondria in control cells showed in the same time frame a more than 3-fold recovery of the fluorescent label, indicating a much larger extent of connectivity of the mitochondrial network. Distinct from mitochondria, the ER network of Drp-1-overexpressing cells showed no alteration in the refilling pattern after bleaching different regions in erGFP-expressing cells.

Division of the Mitochondrial Network Interrupts Intramitochondrial Ca^{2+} Waves and Reduces Mitochondrial Ca^{2+} Uptake

To examine the effect of mitochondrial fragmentation on organelle Ca^{2+} signaling, we applied fast imaging of the ratiometric GFP-based Ca^{2+} probe pericam targeted to mitochondria (2mtRP; Filippin et al., 2003) in HeLa cells expressing only 2mtRP (controls) or coexpressing 2mtRP and Drp-1 (Drp-1-overexpressing cells). Time lapse series of high resolution images were acquired at 5–10 frame(s) and visualized as 2D image series of the whole mitochondrial network (Figure 2A) or linescan images (Figure 2B) along individual mitochondrial profiles

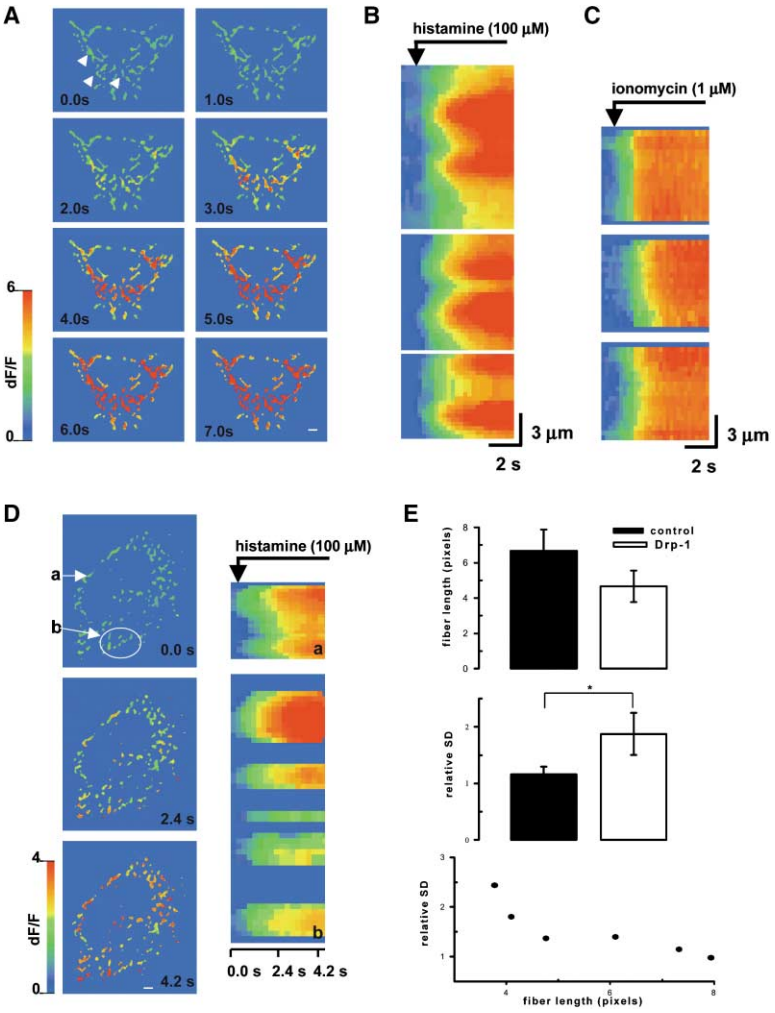

Figure 2. Intramitochondrial Ca^{2+} Waves in the Interconnected Mitochondrial Network and Blockade after Drp-1-Dependent Mitochondrial Division

HeLa cells transiently transfected with the mitochondrially targeted Ca^{2+}-sensitive ratiometric pericam probe 2mtRP were imaged at a rate of 5 frame/sec and stimulated with 100 μM histamine. An image mask acquired from 2D image deconvolution was applied to the image series and relative intensity changes (dF/F) were calculated (see Experimental Procedures and Supplemental Data). (A) 2D representation of timelapse images showing Ca^{2+} waves propagating in the whole mitochondrial network. Elapsed time is shown on each image. Histamine (100 μM) was applied at 1s, Ca^{2+} uptake initiated at isolated sites of the network (see image at 2s), and then the whole mitochondrial network was gradually uploaded. Arrowheads indicate the mitochondria showed by linescan images (see B). (B) Linescan representation (time versus distance in the horizontal and vertical direction, respectively, see bars at lower left corner) of Ca^{2+} waves along mitochondrial profiles (see arrows in [A]), obtained from the 2D images (A). (C) Linescan image of mitochondrial Ca^{2+} uptake after application of the Ca^{2+} ionophore ionomycin (1 μM). Ionomycin caused a homogenous increase along the mitochondrial profiles. Cells are representative of 10–12 measurements from three separate experiments. (D) 2D (left) and linescan (right) representation of $[Ca^{2+}]_m$ changes in the Drp-1-fragmented mitochondrial network. Images are shown before stimulation (0.0 s), at the initiation of mitochondrial Ca^{2+} uptake (2.4 s), and at the time of maximal response (4.2 s). Arrows show a continuous mitochondrial profile (a) and a group of fragmented mitochondria (b), the linescan images of which are displayed. Ca^{2+} wave propagation was observed in (a), but the separate profiles of the fragmented mitochondria in (b) show heterogeneous and spatially limited responses. (E) Quantitative analysis of the 2mtRP image series of the Drp-1-fragmented mitochondrial network, showing reduction of the average fiber length on the 2D mitochondrial profiles (top) and an increase of the relative standard deviation of the $[Ca^{2+}]_m$ response of individual mitochondria in Drp-1-overexpressing cells (middle). Relative SD was calculated as a ratio between SD before and after stimulation (see Experimental Procedures). The lower panels shown the relationship between average fiber length and relative SD measured in each cell. Data are calculated and images are representative of 12 measurements from three separate experiments (asterisk, $p < 0.05$).

(see Supplemental Data at http://www.molecule.org/cgi/content/full/16/1/59/DC1/). In control cells after maximal stimulation with 100 μM histamine, mitochondrial Ca^{2+} uptake initiated at preferential points of the mitochondrial network, and the $[Ca^{2+}]$ increase traveled along the mitochondrial profiles, saturating the relatively high-affinity probe. This pattern was specific for agonist-stimulated Ca^{2+} signals because application of the ionophore ionomycin led to a homogeneous increase through the whole mitochondrial network (Figure 2C). In Drp-1-overexpressing cells, the hot spots of Ca^{2+} uptake were also present, but diffusion of Ca^{2+} waves was limited by the smaller size of mitochondrial particles (Figure 2D). Moreover, even maximal stimulation led to a heterogeneous response of individual mitochondria. In order to quantify the heterogeneity of the $[Ca^{2+}]_m$ responses in controls and Drp-1-overexpressing cells, the standard deviation of the relative fluorescence changes over individual mitochondrial objects was calculated showing a significantly higher value in Drp-1-overexpressing cells (1.16 ± 0.13 in controls versus 1.87 ± 0.37 in Drp-1-overexpressing cells, $p < 0.05$; Figure 2E). The heterogeneity of the response showed a reverse correlation with the average fiber length (Figure 2E).

To assess the average mitochondrial Ca^{2+} load of individual cells during agonist stimulation, we applied the FRET-based mitochondrially targeted Ca^{2+} sensitive probe yellow cameleon (2mtYC2.1; Filippin et al., 2003), which has lower Ca^{2+} affinity than 2mtRP and thus is more suitable for quantitative assessment of the high $[Ca^{2+}]_m$ responses. As shown in Figure 3, we observed a reduction of the peak responses in Drp-1-overexpressing cells (normalized ratio values: 1.33 ± 0.03 in control versus 1.25 ± 0.03 in Drp-1-overexpressing cells, $p < 0.05$; Figure 3A). Interestingly, most probably due to the reduced overall volume and increased surface/volume ratio of the smaller mitochondrial particles in Drp-1-overexpressing cells, detailed analysis of the Ca^{2+} up-

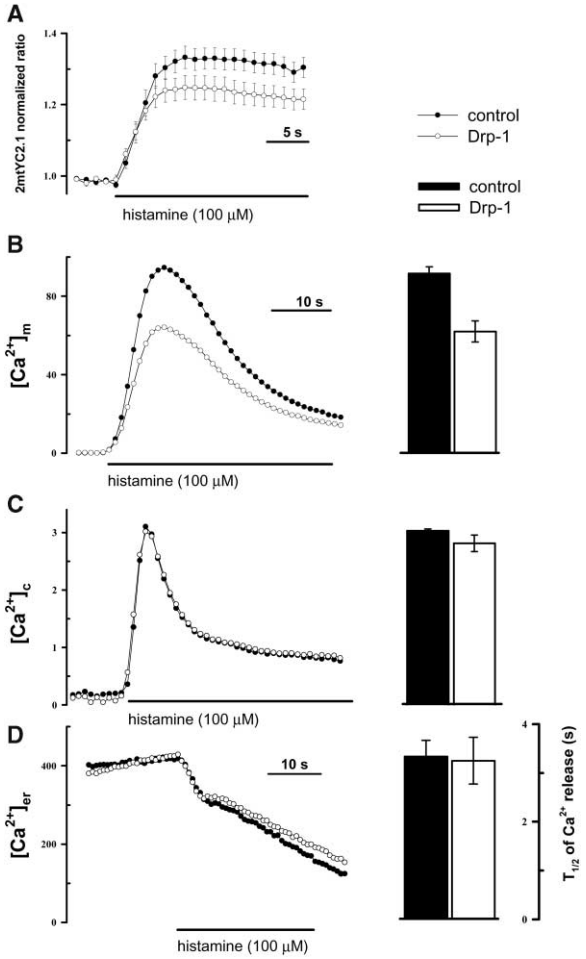

Figure 3. Drp-1-Dependent Mitochondrial Division Reduces the Average Agonist-Induced $[Ca^{2+}]_m$ Uptake

(A) $[Ca^{2+}]_m$ response to 100 μM histamine in HeLa cells transfected with the 2mtYC2.1 Ca^{2+} probe (control) and co-transfected with the probe and Drp-1 (Drp-1-overexpressing cells). Cells were microperfused in an extracellular buffer (KRB/Ca^{2+}) in a thermostatted chamber at 37°C and stimulated with 100 μM histamine. Emission ratio images were obtained at 440 nm excitation and 510/20 nm (YFP) and 460/20 nm (CFP) emission, and average ratios from whole cells were normalized to control levels.

(B–D) $[Ca^{2+}]$ measurements of different cellular compartments of HeLa cells transfected with specifically targeted aequorin probes ([B]: mitochondria, mtAEQmut; [C]: cytosol, cytAEQ; [D]: ER, erAEQmut [Chiesa et al., 2001]). Control cells were transfected only with the recombinant Ca^{2+} probe of interest (filled circles and bars), or cotransfected with Drp-1 (open circles and bars). Aequorin luminescence was measured in a population of transfected cells seeded on coverslips and perfused at 37°C with KRB/Ca^{2+}. Luminescence data were converted to $[Ca^{2+}]$ (see Experimental Procedures). Cells were stimulated with 100 μM histamine where indicated. On the left, representative data of >12 traces obtained from at least three separate experiments; on the right, mean peak values of the $[Ca^{2+}]_m$ and $[Ca^{2+}]_c$ responses and average velocity of ER Ca^{2+} release is shown on the same ordinate axis.

take kinetics revealed an increased initial uptake rate in these mitochondria (Supplemental Figure S2). However, this effect was masked by the heterogeneity of mitochondrial Ca^{2+} responses in single cell experiments and by the lower time resolution applied in population measurements.

To fully assess the change in mitochondrial Ca^{2+} responses caused by organelle fragmentation, we carried out a series of experiments with targeted aequorin chimeras. Specifically, we employed recombinant aequorins targeted to the mitochondria, cytosol, and ER (cytAEQ, erAEQmut, and mtAEQmut, respectively; Chiesa et al., 2001). In agreement with the data obtained with the 2mtYC2.1 probe, the peak $[Ca^{2+}]_m$ response was significantly reduced in Drp-1-overexpressing cells (91.7 ± 6.8 μM in control versus 62.2 ± 5.4 μM in Drp-1-overexpressing cells, $p < 0.01$) as measured by the low-affinity mtAEQmut probe (Figure 3B). The reduction of mitochondrial Ca^{2+} responses was not a consequence of changes in global Ca^{2+} signaling. Indeed, neither $[Ca^{2+}]_c$ responses nor $[Ca^{2+}]_{er}$ steady-state level and Ca^{2+} release kinetics were altered (Figures 3C and 3D). No alteration was detected also in single cell imaging experiments in fura-2-loaded control and Drp-1-overexpressing cells (Supplemental Figure S2).

In order to investigate the possibility that the change of the average mitochondrial particle size had an effect in itself on the driving force for mitochondrial Ca^{2+} uptake (e.g., by changing the surface/volume ratio), we measured the mitochondrial membrane potential ($\Delta\Psi_m$) by estimating the steady-state loading of TMRM into mitochondria of control and Drp-1-overexpressing cells. The average $\Delta\Psi_m$ of the two groups of cells showed no difference (Supplemental Figure S3B). Moreover, correlation analysis between mitochondrial particle size and TMRM loading showed that the reduction of mitochondrion size did not alter $\Delta\Psi_m$, since the correlation coefficient between mitochondrial size and TMRM intensity was very low ($r^2 = 0.072 \pm 0.04$; Supplemental Figure S3D). Similarly, heterogeneity in $\Delta\Psi_m$ did not increase in Drp-1-expressing cells, as assessed by the analysis of the average standard deviation of TMRM intensity in particles of the normal and fragmented mitochondrial network (Supplemental Figure S3C). Thus, we concluded that the heterogeneity of Ca^{2+} uptake observed in cells having a fragmented mitochondrial network was not due to a reduced driving force for Ca^{2+} influx (and thus inefficient ER/mitochondria contacts), but rather to the impairment of intramitochondrial Ca^{2+} diffusion.

The Amplitude of the $[Ca^{2+}]_m$ Rise Depends on Intramitochondrial Ca^{2+} Diffusion and the Number of ER-Mitochondrial Ca^{2+} Transmission Sites

In view of intramitochondrial diffusion of Ca^{2+} waves, we envisioned the possibility that stimulation of the cells with submaximal agonist concentration might lead not only to decreased average $[Ca^{2+}]_m$ elevation but also to heterogeneous $[Ca^{2+}]_m$ responses in different areas of the mitochondrial network. Indeed, as measured by 2mtRP, application of 5 μM histamine led to Ca^{2+} increases at preferential Ca^{2+} uptake sites in control cells, but the diffusion of Ca^{2+} was limited, and thus the $[Ca^{2+}]_m$ rise did not extend to the whole network. Only the subsequent addition of a maximal histamine dose converted these local Ca^{2+} increases into diffusing Ca^{2+} waves (Figure 4A). Thus, we concluded that in fragmented mitochondrial network of Drp-1-overexpressing cells, showing similar heterogeneity and a lower average $[Ca^{2+}]_m$

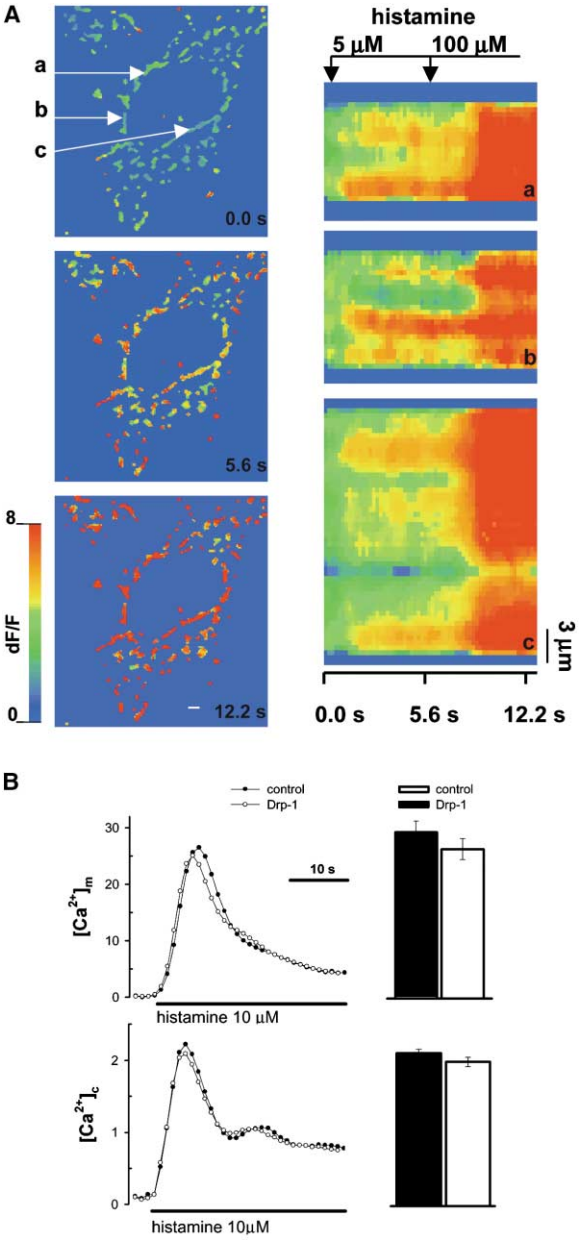

Figure 4. Submaximal Agonist Stimulation Leads to a Heterogeneous $[Ca^{2+}]_m$ Response, which Is Unaffected by Drp-1-Dependent Mitochondrial Division

(A) HeLa cells were transiently transfected with 2mtRP, and images were acquired during stimulation with different histamine concentrations and analyzed as described in Figure 2 (see also Experimental Procedures and Supplemental Data). 2D (left) and linescan (right) representation of $[Ca^{2+}]_m$ changes of the continuous mitochondrial network in response to subsequent application of 5 μM and 100 μM histamine. Images are shown before stimulation (0.0 s), after application of 5 μM histamine (5.6 s), and at maximal stimulation (12.2 s). Arrows show different mitochondrial profiles applied to linescan analysis (a, b, and c), showing limited response to 5 μM and spreading of Ca^{2+} at 100 μM histamine stimulation. The cell shown is representative of ten measurements from three separate experiments. Scalebar, 5 μm.

(B) $[Ca^{2+}]$ measurements in the mitochondrial and cytosolic compartments of HeLa cells transfected with targeted aequorin probes (top: mitochondria, mtAEQmut; bottom: cytosol, cytAEQ). Control cells were transfected only with the aequorin probe (filled circles and bars) or cotransfected with Drp-1 (open circles and bars). Aequorin luminescence was measured and calibrated as in Figure 3 (see also Experimental Procedures). The left panels show representative data of >12 traces obtained from three separate experiments. Right panels show the mean peak values of the $[Ca^{2+}]_m$ and $[Ca^{2+}]_c$ responses from the same set of data.

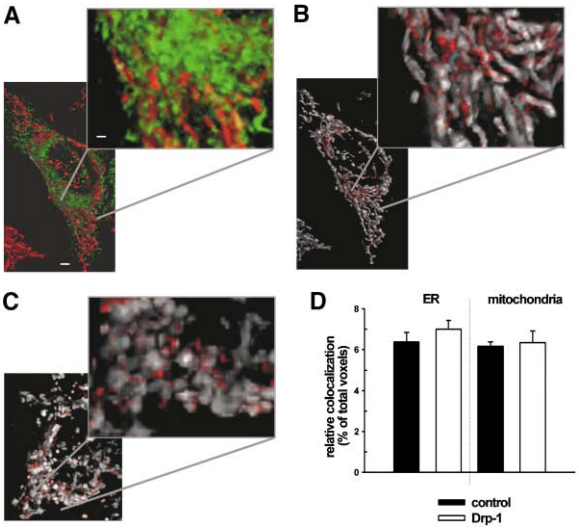

Figure 5. Drp-1-Induced Mitochondrial Fragmentation Does Not Change the Number of ER-Mitochondria Contacts

HeLa cells were transiently transfected with erGFP (control, A and B) or erGFP and Drp-1 (Drp-1-overexpressing cells, D) and loaded with MitoTracker Red (see Experimental Procedures and Supplemental Data). The two deconvolved image series, acquired by digital microscopy (see also Figure 1), were superimposed after 3D reconstruction and colocalization was quantitatively analyzed. (A) Superimposed 3D reconstructed images of the ER and mitochondrial network. (B) and (C) Representation of the mitochondrial surface showing colocalization with the ER in control (B) and Drp-1-fragmented network (D). The mitochondrial network is shown in grayscale, and only the ER-colocalizing voxels appear in red on top of the mitochondrial surface. (D) Quantitative colocalization analysis (for details see Experimental Procedures) reveals no difference between control (filled bars) and Drp-1-overexpressing cells (open bars) in the relative colocalizing voxels neither in the ER nor in the mitochondrial network. Data are obtained from 12 cells examined from three separate experiments.

elevation even at maximal stimulation, Ca^{2+} waves could not reach a number of individual mitochondria due to the lack of connectivity. Accordingly, at submaximal stimulation (10 μM histamine), Drp-1 overexpression did not significantly modify the $[Ca^{2+}]_m$ peak (29.2 ± 2.95 μM in controls versus 26.24 ± 2.85 μM in Drp-1-overexpressing cells, $p > 0.2$), as measured in cell population with the mtAEQmut probe (Figure 4B).

Finally, we needed to rule out another possible explanation for the reduction of $[Ca^{2+}]_m$ rises in Drp-1-overexpressing cells, i.e., that the number of Ca^{2+} uptake sites is reduced during the forced division of the mitochondrial network. To examine the total number of these preferential Ca^{2+} uptake sites in the whole cell volume, we analyzed the colocalization between mitochondria and ER with 3D reconstructed images of erGFP and MitoTracker Red in control (transfected only with erGFP) and Drp-1-overexpressing (cotransfected with erGFP and Drp-1) cells (Figure 5). We assumed that the colocal-

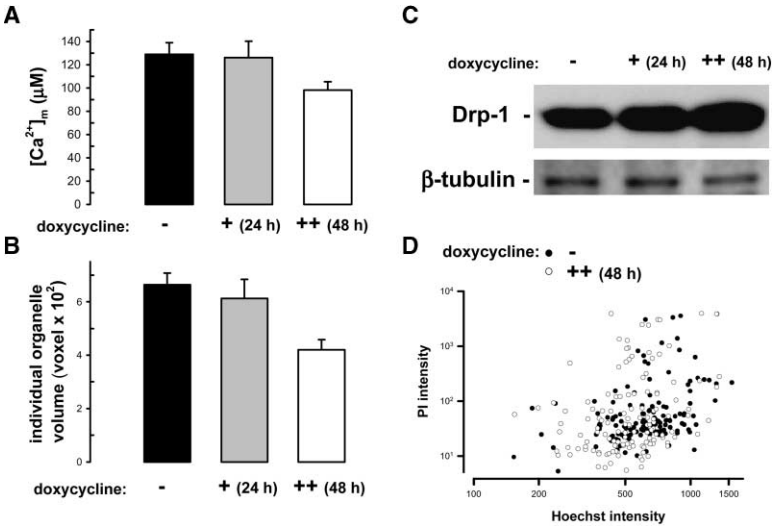

Figure 6. Dose-Dependent Effect of Drp-1 Overexpression on Mitochondrial Division, Ca^{2+} Signaling, and Cell Viability

The inducible clone T-Rex-Drp-1 was used with different induction time and concentration of doxycycline (1 μg/mL for 24 hr or 2 μg/mL for 48 hr, plus symbol and double plus symbol, respectively). (A) Effect of different inductions on the mitochondrial Ca^{2+} signal evoked by 100 μM histamine. Cells were transfected with mtAEQmut, and 36 hr after transfection, $[Ca^{2+}]_m$ was measured as described in Figure 4 (see also Experimental Procedures). The mean of peak responses of ten measurements from three separate experiments is shown. (B) Morphological analysis of the mitochondrial network of T-Rex-Drp-1 cells labeled with MitoTracker Red. Images were acquired by digital microscopy, deconvolved, and 3D reconstructed (see Figure 1 and Experimental Procedures). The result of measurements of average individual organelle volume from ten cells for each group with different induction is shown. (C) Western blot analysis of Drp-1 expression in T-Rex-Drp-1 cells after different inductions. The amount of β-tubulin is shown as control. (D) Effect of strong Drp-1 induction (2 μg/mL, 48 hr) on cell viability. After induction, cells were loaded with Hoechst and propidium iodide (PI), and the intensity of nuclear and whole-cell fluorescence was measured in ~2–300 cells/experiment to assess apoptotic nuclear condensation and necrotic plasmamembrane rupture, respectively. The fluorescence values of Hoechst versus PI were plotted for each cell, showing equal distribution before and after Drp-1 induction. A representative distribution from three experiments is shown.

izing ER and mitochondrial spots represent the sites of the most efficient Ca^{2+} signal transmission between the two organelles matching the requirements for the activation of the MCU. Despite the significant fragmentation of the mitochondrial network in Drp-1-overexpressing cells, the average number and volume of contact sites remained unaltered (Figure 5D), also implying that a significant number of mitochondrial fragments remained without direct connection to mitochondrial Ca^{2+} uptake sites.

Consequences of Drp-1-Induced Mitochondrial Scission for Ca^{2+}-Mediated and Ca^{2+}-Independent Apoptosis

Since Drp-1 was shown to be involved in mitochondrial translocation of proapoptotic proteins (e.g., Bax [Frank et al., 2001; Karbowski et al., 2002; Breckenridge et al., 2003]) at potential scission sites of the mitochondrial network, we investigated the effect of its overexpression on cell viability/apoptosis in intact (nontreated) cells. In these experiments, we used the inducible T-Rex-Drp-1 clone (Karbowski et al., 2002) in which the expression level of the protein can be regulated by varying the time of induction by tetracycline/doxycycline (that derepresses the synthesis of the protein) as well as by varying its concentration. As shown in Figure 6, only strong induction of Drp-1 was accompanied by significant division of the network and reduction of the mean mitochondrial Ca^{2+} uptake (peak response after 100 μM histamine stimulation: 128.7 ± 10.1 μM in noninduced cells versus 98.1 ± 7.0 μM after induction). Remarkably, even the strong induction of Drp-1 could not increase the number of cells either with chromatin condensation or PI accumulation, showing that substantial Drp-1 overexpression and increased mitochondrial division does not induce, by itself, necrotic or apoptotic cell death (Figure 6D).

To investigate the effect of mitochondrial fragmentation and thus reduced overall mitochondrial Ca^{2+} uptake on Ca^{2+}-mediated apoptotic pathways, we used serum deprivation, exogenously added C_2 ceramide, or H_2O_2 treatment, all inducing Ca^{2+} release and mitochondrial Ca^{2+} overload (Wang et al., 1995; Scorrano et al., 2003). To investigate the involvement of Ca^{2+}-independent mitochondrial pathways, we used staurosporine treatment and Bax overexpression, exerting direct effect on OMM permeability (Scorrano and Korsmeyer, 2003).

While the induction of Drp-1 in the T-Rex-Drp-1 HeLa cell clone in itself did not modify the basal cytoplasmic cytochrome c level, it reduced the amount of cytochrome c released by serum deprivation and treatment of the cells with 500 μM H_2O_2 (Figure 7A). In contrast, cytochrome c release induced by staurosporine was slightly increased after induction of Drp-1 expression, in agreement with previous reports (Frank et al., 2001). As for late apoptotic events (Figure 7B), Drp-1 induction caused reduction of caspase 3 activity after C_2 ceramide treatment, while caspase 3 activation was potentiated in staurosporine treated cells.

To study the final outcome of cell death in response to these two groups of apoptotic stimuli, we assessed cell survival by combining phase contrast and fluorescent microscopy. HeLa cells were transiently transfected with mitochondrially targeted dsRed (mtdsRed) alone (controls) or in combination with Drp-1 (Drp-1-overexpressing cells). To evaluate the Ca^{2+}-dependent pathway, two different concentrations of C_2 ceramide (2 μM and 10 μM) were directly applied to the cells. After 12 hr of treatment, the ratio of transfected cells to the total number of surviving cells was calculated (Figure 7C). In this experimental setup, positive changes in the percentage of transfected cells indicates protection against the apoptotic stimulus by the overexpressed protein, while reduction provides evidence for its proapoptotic effect (Pinton et al., 2001). At low C_2 ceramide

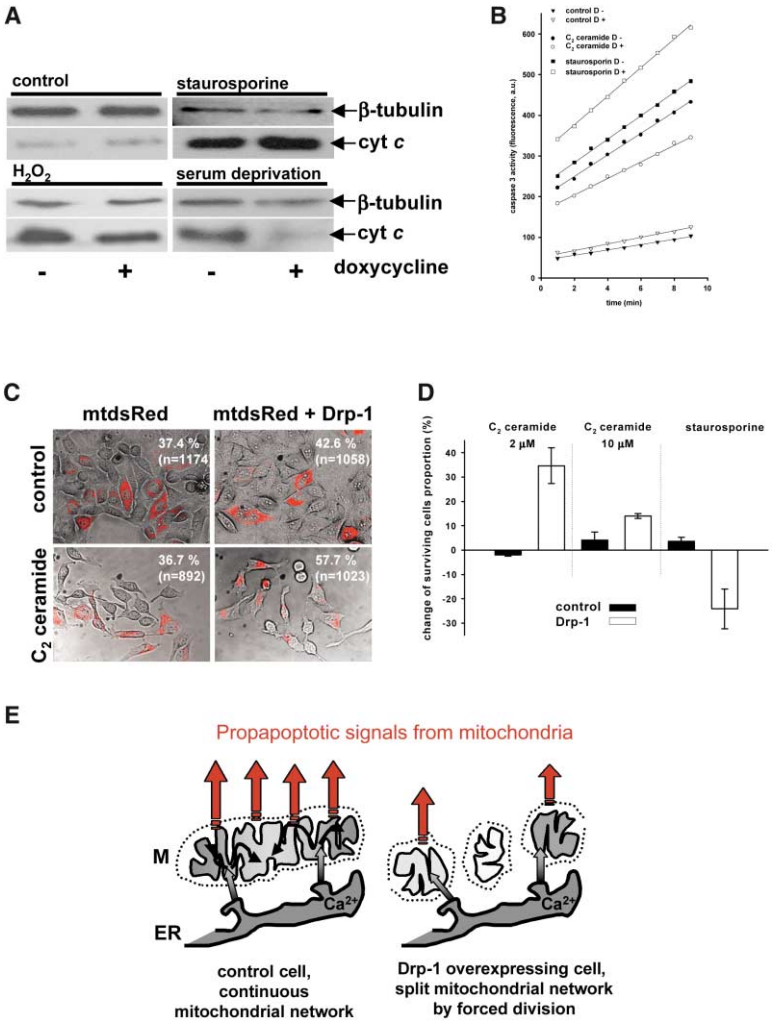

Figure 7. Drp-1-Induced Mitochondrial Division Protects Selectively against Ca^{2+}-Mediated Apoptosis

(A) Western blot analysis of cytochrome c, present in the cytosolic compartment in T-Rex-Drp-1 HeLa cells with and without induction of Drp-1 expression with doxycycline (2 μg/mL, 48 hr). Cytosolic cytochrome c levels were analyzed in control (nontreated) cells and after staurosporine (6 hr), H_2O_2 (12 hr) addition, and serum deprivation (16 hr) and compared to endogenous β-tubulin levels.

(B) Caspase-3-like activity measured by the production of the rhodamine-labeled Z-DEVD-R110 compound from cell extracts of the T-Rex-Drp-1 HeLa clone without (D−) and with (D+) induction of Drp-1 expression with doxycycline (2 μg/mL, 48 hr). Control activities (triangles) were measured in the presence of the Ac-DEVD-CHO caspase inhibitor; two other group of cells were treated for 6 hr with 1 μM staurosporine (squares) and 60 μM C_2 ceramide (circles).

(C) The sensitivity of control and Drp-1-overexpressing HeLa cells to different apoptotic stimuli was measured by transiently transfecting them with mitochondrial DsRed (mtDsRed, control cells) and mtDsRed with Drp-1 and exposing them to C_2 ceramide (2 and 10 μM, 12 hr) and staurosporine (1 μM, 5 hr). Representative overlays of phase contrast and red fluorescent images of control (left) and Drp-1-overexpressing (right) cells without treatment and after treatment with 2 μM C_2 ceramide are shown. The percentage of transfected cells is written on the image in each condition (number of cells examined in three separate experiments is shown in parentheses). Note the increased proportion of surviving Drp-1-transfected cells (lower right) after C_2 ceramide treatment.

(D) Relative changes of the percentage of surviving transfected cells after C_2 ceramide and staurosporine treatment compared to nontreated cells. Positive values of Drp-1-overexpressing cells represent protection against C_2 ceramide-induced apoptosis, while negative values denote potentiation of the proapoptotic effect of staurosporine.

(E) Model of Ca^{2+} and apoptotic signaling in the connected, tubular mitochondrial network and in the mitochondrial network after forced division.

concentration, we observed a substantial increase in the proportion of Drp-1-expressing cells (an increase by 34.7% ± 7.3%, $p < 0.02$ in Drp-1-overexpressing cells versus –2.0% ± 0.5% in controls as compared to nontreated cells), and a smaller protecting effect was also observed at high C_2 ceramide concentration (an increase by 14.1% ± 1.0%, $p < 0.05$ in Drp-1-overexpressing cells versus 4.15% ± 3.3% in controls as compared to nontreated cells, Figure 7D). As expected, no change in the percent of fluorescent cells was detected in control cells (transfected only with mtdsRed), since in this case the recombinantly expressed protein exerts no protection from the apoptotic stimulus. These results further confirmed that mitochondrial division increases the threshold for apoptosis induction by ER Ca^{2+} release and mitochondrial overload caused by C_2 ceramide. Moreover, this outcome was restricted to this particular apoptotic pathway, since, in agreement with previous data (Karbowski et al., 2002), Drp-1 overexpression significantly potentiated the effect of staurosporine (a decrease of fluorescent cells by 24.1% ± 8.12% in Drp-1-overexpressing cells versus 3.6% ± 1.7% in controls as compared to nontreated cells, $p < 0.05$), a proapoptotic agent that directly targets mitochondria (Figure 7D). Similarly, transfection of the T-Rex-Drp-1 clone with Bax and mtdsRed and assessment of the transfected cell proportion showed a decrease of the percentage of transfected cells after Drp-1 induction (data not shown). Thus, also in this case a potentiating effect of Drp-1 on the Ca^{2+}-independent mitochondrial pathway induced by Bax overexpression can be inferred.

Discussion

The Nature of Intramitochondrial Ca^{2+} Signaling

Recently, the use of targeted recombinant aequorin probes revealed that upon agonist stimulation an efficient mitochondrial Ca^{2+} signal, generally in the 5–100 μM range, follows a much lower cytoplasmic [Ca^{2+}] elevation (Rizzuto et al., 1998). The development of GFP-based Ca^{2+} probes allowed acquisition of spatial information about organelle Ca^{2+} signaling (Miyawaki, 2003).

Here, using both targeted aequorins and GFP-based probes (2mtRP and 2mtYC2.1), we concluded that the intramitochondrial Ca^{2+} signal shows an inherent heterogeneity, since Ca^{2+} uptake from the extramitochondrial space originates from a limited number of sites in the intact tubular network and intraorganellar Ca^{2+} diffusion is required for the maximal $[Ca^{2+}]_m$ response. These preferential sites either represent the close apposition of mitochondria to the high $[Ca^{2+}]$ microdomains formed at the mouth of Ca^{2+} release sites of the $InsP_3$ receptors residing in the ER or may be the consequence of clustering of MCU, probably at the same sites. Regardless of their nature, they are located at a relatively long distance, thus division of the mitochondrial network generates individual mitochondrial particles devoid of connections to Ca^{2+} sources. This, in turn, results in increased heterogeneity in the $[Ca^{2+}]_m$ elevation throughout the mitochondrial network and in overall reduction of the mitochondrial Ca^{2+} load.

The Role of Drp-1 in Mitochondrial Division

The key role of Drp-1 in mitochondrial division was shown by morphological and functional studies using its dominant-negative mutant Drp-1^{K38A} (Smirnova et al., 2001). However, although overexpression of wild-type Drp-1 increased mitochondrial division in *C. elegans* (Labrousse et al., 1999), it did not affect markedly mitochondrial morphology in mammalian cells (Legros et al., 2002). Our experiments confirmed this notion by showing a marked effect on mitochondrial morphology only at very high expression levels. This may also indicate that the availability of anchoring proteins in the OMM, such as hFis1 in humans, is a rate-limiting step for Drp-1 activity (James et al., 2003).

The Role of Drp-1 in Targeting Proapoptotic Members of the Bcl-2 Family to Mitochondria

Mitochondrial fragmentation, which occurs in several apoptotic models, has been directly implicated in the transduction of apoptotic signals involving OMM permeabilization (Karbowski et al., 2002; Breckenridge et al., 2003). Drp-1 was detected in complexes at mitochondrial fission sites with Bax, mediating OMM permeabilization and cytochrome c release (Harris and Thompson, 2000). Moreover, Drp-1 overexpression amplified Bax-mediated release of cytochrome c induced by staurosporine (Scorrano and Korsmeyer, 2003). Conversely, expression of the GTPase mutant Drp-1^{K38A} prevented mitochondrial scission and cell death, without inhibiting Bax translocation to the OMM. It was suggested that morphological alteration induced by Drp-1 leads to OMM permeabilization (Gottlieb et al., 2003). However, our results demonstrate that even a large overproduction of Drp-1 followed by a significant fragmentation of the mitochondrial network was not accompanied by cell death induction, though it clearly increased the susceptibility to Bax-mediated, staurosporine-induced apoptosis. Further studies are needed to clarify the role of additional components (possibly present in complex with Bax/Drp-1/hFis1) in OMM permeabilization (Karbowski and Youle, 2003).

The Role of Drp-1-Mediated Mitochondrial Division in Ca^{2+}-Mediated Apoptosis

Recent evidence validated Ca^{2+} as a key effector in the apoptotic response induced by stimuli like C_2 ceramide, H_2O_2, or arachidonic acid (for review see Hajnoczky et al. [2003] and Rizzuto et al. [2003]). These stimuli induce movement of Ca^{2+} from the endoplasmic reticulum to mitochondria, leading to Ca^{2+} overload, OMM permeabilization, and caspase-mediated cell death (Bernardi, 1999). The oncoprotein Bcl-2, by decreasing the releasable ER Ca^{2+} pool, was shown to reduce mitochondrial Ca^{2+} uptake (Pinton et al., 2000). Conversely, the ER resident fraction of Bax increased $[Ca^{2+}]_{er}$, thus amplifying Ca^{2+}-mediated cell death (Scorrano et al., 2003; Zong et al., 2003). Here, we present new evidence from the mitochondrial side, i.e., an overall reduction of the $[Ca^{2+}]_m$ response after ER Ca^{2+} release has an antiapoptotic effect as well. Since mitochondrial Ca^{2+} uptake sites appear to be spatially dispersed also in cells having an intact mitochondrial network, an important consequence of the breakdown of the tubular mitochondrial network is that a substantial number of mitochondrial fragments apparently remain without direct sources of Ca^{2+} supply, thus they are not exposed to Ca^{2+} overload during the apoptotic process. Interestingly, these data appear to match those of Hajnoczky and coworkers (Pacher and Hajnoczky, 2001), who showed Ca^{2+}-dependent waves of mitochondrial depolarization in permeabilized cells treated with ceramide. In this case the waves were slower, suggesting a delay between the Ca^{2+} rise and depolarization, although other possibilities, such as the loss of a sensitizing factor in permeabilized cells, cannot be excluded.

In conclusion, we propose a model (Figure 7E) in which Drp-1-mediated division regulates luminal connectivity of the mitochondrial network, and this regulation serves to adapt mitochondria to cell stress by modifying mitochondrial Ca^{2+} uptake. The efficiency of mitochondrial Ca^{2+} accumulation depends on propagation of Ca^{2+} waves in the mitochondrial matrix, since primary Ca^{2+} uptake occurs at separate and distant sites of the network and filling of the whole network is ensured by lateral Ca^{2+} diffusion. Division of the mitochondrial network leads to the positioning of mitochondrial particles far from sources of Ca^{2+} release (ER), thus reducing the average Ca^{2+} uptake efficiency. This reduction may still ensure Ca^{2+}-dependent homeostatic functions of mitochondria, as it does not confer reduction of cell viability but also serves as a protection in stress responses involving ER/mitochondrial Ca^{2+} crosstalk, mitochondrial Ca^{2+} overload, and consequent cell death induction. In this scenario, the process of mitochondrial fusion/fission emerges as an important regulator of mitochondrial signaling properties and of the broadly different intracellular effects of physiological and pathological stimuli.

Experimental Procedures

Cell Culture and Transfection

HeLa cells were cultured in DMEM supplemented with 10% FCS. For aequorin measurements, cells were cotransfected with Drp-1/pcDNA3.1 (Smirnova et al., 1998; Frank et al., 2001) and cytAEQ/VR1012, erAEQmut/pcDNA1, or mtAEQmut/VR1012 as previously described (Chiesa et al., 2001). For imaging experiments, cells were

cotransfected with Drp-1/pcDNA3.1 and 2mtYC2.1, 2mtRP (Filippin et al., 2003), erGFP/VR1012 (Chiesa et al., 2001), or mitochondrially targeted dsRed (mtdsRed, Clontech, Palo Alto, CA). Transient transfection was done by the Ca^{2+}-phosphate precipitation technique. Experiments were carried out 24–36 hr after transfection. The T-Rex-Drp-1 HeLa clone (Karbowski et al., 2002) was cultured in MEM containing 10% FCS, and imaging and aequorin measurements were carried out as in wild-type HeLa cells. Drp-1 induction was achieved by supplementing the culture medium with doxycycline (1 μg/mL for 24 hr or 2 μg/mL for 48 hr).

Aequorin Measurements

CytAEQ-, mtAEQmut-, or erAEQmut-expressing cells were reconstituted with coelenterazine and transferred to the perfusion chamber. The light signal was collected in a purpose-built luminometer and calibrated into $[Ca^{2+}]$ values as previously described (Chiesa et al., 2001). All aequorin measurements were carried out in KRB-containing 1 mM $CaCl_2$ (KRB/Ca^{2+}, Krebs-Ringer modified buffer: 135 mM NaCl, 5 mM KCl, 1 mM $MgSO_4$, 0.4 mM K_2HPO_4, 1 mM $CaCl_2$, 5.5 mM glucose, and 20 mM HEPES [pH 7.4]).

Imaging Procedures

For mitochondrial and cytosolic $[Ca^{2+}]$ imaging, HeLa cells were transfected with 2mtYC2.1 or 2mtRP ± Drp-1/pcDNA3.1 and/or loaded with 4 μM fura-2 AM. For measurement of $\Delta\Psi_m$, cells were loaded with 10 nM tetramethylrhodamine methyl ester (TMRM). For 3D morphological image acquisition, the cells were transfected with erGFP/VR1012 and loaded with 40 nM MitoTracker Red 580 (all dyes were from Molecular Probes, Leiden, Netherlands). All imaging experiments were carried out on Zeiss Axiovert 200 inverted microscopes equipped either with cooled CCD digital cameras or as part of the Zeiss LSM 510 confocal microscope (Carl Zeiss, Jena, Germany). For details of the imaging systems and the applied protocols for image acquisition and processing, see the Supplemental Data.

Apoptosis Detection

For combined detection of apoptotic and necrotic cell death, T-Rex-Drp-1 cells were loaded simultaneously with Hoechst 33342 (Molecular Probes, Leiden, Netherlands) and propidium iodide for 5 min. Z-series images of labeled cells were acquired by digital imaging (see above), and the intensity of the two dyes in each cell was quantified on maximal projection images. Caspase-3-like activity was evaluated with the EnzChek caspase-3 assay kit 2 (Molecular Probes) according to the recommended protocol; the amount of assayed proteins was quantified by standard Bradford assay. Enzymatic activity was determined spectrofluorimetrically (L550B Perkin Elmer spectrometer) by measuring the kinetics of fluorescence increase at excitation/emission wavelengths of 496/520 nm.

Western Blot Analysis

T-Rex-Drp-1 cells were plated in 10 cm Petri dishes. After Drp-1 induction, cells were washed twice in PBS, scraped, centrifuged (1,000 rpm, 5 min, room temperature), resuspended, and homogenized (10 mM NaCl, 10 mM Tris-HCl, 1 mM EDTA, 1 mM EGTA, 1 mM DTT, and protease inhibitor cocktail [pH 7.4; Sigma-Aldrich]). Subcellular fractionation was performed as previously described (Chami et al., 2003). The proteins were separated by SDS-PAGE on a 10% gel, and the amount of Drp-1, cytochrome c, and β-tubulin was estimated by Western blotting with mouse anti-DLP1 (1:5,000; BD Biosciences, Pharmingen), mouse anti-cytochrome c, mouse anti-β-tubulin (1:5,000; Santa Cruz Biotechnology), primary antibodies, and anti-mouse IgG HRP-labeled secondary antibodies (1:10,000; Santa Cruz Biotechnology), according to standard protocols.

Statistical data are presented as mean ± S.E.M., significance was calculated by Student's t test, and correlation analysis was done with the SigmaPlot 5.0 software (SPSS Inc.).

Acknowledgments

We thank Doctors E. Rapizzi and K.E. Fogarty and Crisel Instruments (Roma, Italy) for their valuable help in image acquisition and analysis, and Dr. M. Rojo for providing the Drp-1/pCB6 cDNA. This work was supported by grants from Telethon-Italy (Grants numbers 1285 and GTF02013), the Italian Association for Cancer Research (AIRC), the Human Frontier Science Program, the Italian University Ministry (MURST and FIRB), and the Italian Space Agency (ASI). M.R.W. and M.C. are recipients of FEBS and EMBO long-term fellowships, respectively. Part of the work by G.S. was supported by a Marie-Curie individual fellowship (HPMF-CT-2000-00644).

Received: February 28, 2004
Revised: July 21, 2004
Accepted: August 10, 2004
Published: October 7, 2004

References

Bernardi, P. (1999). Mitochondrial transport of cations: channels, exchangers, and permeability transition. Physiol. Rev. *79*, 1127–1155.

Breckenridge, D.G., Stojanovic, M., Marcellus, R.C., and Shore, G.C. (2003). Caspase cleavage product of BAP31 induces mitochondrial fission through endoplasmic reticulum calcium signals, enhancing cytochrome c release to the cytosol. J. Cell Biol. *160*, 1115–1127.

Chami, M., Ferrari, D., Nicotera, P., Paterlini-Brechot, P., and Rizzuto, R. (2003). Caspase-dependent alterations of Ca2+ signaling in the induction of apoptosis by hepatitis B virus X protein. J. Biol. Chem. *278*, 31745–31755.

Chiesa, A., Rapizzi, E., Tosello, V., Pinton, P., de Virgilio, M., Fogarty, K.E., and Rizzuto, R. (2001). Recombinant aequorin and green fluorescent protein as valuable tools in the study of cell signaling. Biochem. J. *355*, 1–12.

Csordas, G., Thomas, A.P., and Hajnoczky, G. (1999). Quasi-synaptic calcium signal transmission between endoplasmic reticulum and mitochondria. EMBO J. *18*, 96–108.

Duchen, M.R. (2000). Mitochondria and calcium: from cell signaling to cell death. J. Physiol. *529*, 57–68.

Filippin, L., Magalhaes, P.J., Di Benedetto, G., Colella, M., and Pozzan, T. (2003). Stable interactions between mitochondria and endoplasmic reticulum allow rapid accumulation of calcium in a subpopulation of mitochondria. J. Biol. Chem. *278*, 39224–39234.

Frank, S., Gaume, B., Bergmann-Leitner, E.S., Leitner, W.W., Robert, E.G., Catez, F., Smith, C.L., and Youle, R.J. (2001). The role of dynamin-related protein 1, a mediator of mitochondrial fission, in apoptosis. Dev. Cell *1*, 515–525.

Gottlieb, E., Armour, S.M., Harris, M.H., and Thompson, C.B. (2003). Mitochondrial membrane potential regulates matrix configuration and cytochrome c release during apoptosis. Cell Death Differ. *10*, 709–717.

Hajnoczky, G., Davies, E., and Madesh, M. (2003). Calcium signaling and apoptosis. Biochem. Biophys. Res. Commun. *304*, 445–454.

Harris, M.H., and Thompson, C.B. (2000). The role of the Bcl-2 family in the regulation of outer mitochondrial membrane permeability. Cell Death Differ. *7*, 1182–1191.

James, D.I., Parone, P.A., Mattenberger, Y., and Martinou, J.C. (2003). hFis1, a novel component of the mammalian mitochondrial fission machinery. J. Biol. Chem. *278*, 36373–36379.

Karbowski, M., and Youle, R.J. (2003). Dynamics of mitochondrial morphology in healthy cells and during apoptosis. Cell Death Differ. *10*, 870–880.

Karbowski, M., Lee, Y.J., Gaume, B., Jeong, S.Y., Frank, S., Nechushtan, A., Santel, A., Fuller, M., Smith, C.L., and Youle, R.J. (2002). Spatial and temporal association of Bax with mitochondrial fission sites, Drp1, and Mfn2 during apoptosis. J. Cell Biol. *159*, 931–938.

Kirichok, Y., Krapivinsky, G., and Clapham, D.E. (2004). The mitochondrial calcium uniporter is a highly selective ion channel. Nature *427*, 360–364.

Labrousse, A.M., Zappaterra, M.D., Rube, D.A., and van der Bliek, A.M. (1999). C. elegans dynamin-related protein DRP-1 controls severing of the mitochondrial outer membrane. Mol. Cell *4*, 815–826.

Legros, F., Lombes, A., Frachon, P., and Rojo, M. (2002). Mitochondrial fusion in human cells is efficient, requires the inner membrane

potential, and is mediated by mitofusins. Mol. Biol. Cell *13*, 4343–4354.

McCormack, J.G., Halestrap, A.P., and Denton, R.M. (1990). Role of calcium ions in regulation of mammalian intramitochondrial metabolism. Physiol. Rev. *70*, 391–425.

Miyawaki, A. (2003). Fluorescence imaging of physiological activity in complex systems using GFP-based probes. Curr. Opin. Neurobiol. *13*, 591–596.

Mozdy, A.D., and Shaw, J.M. (2003). A fuzzy mitochondrial fusion apparatus comes into focus. Nat. Rev. Mol. Cell Biol. *4*, 468–478.

Orrenius, S., Zhivotovsky, B., and Nicotera, P. (2003). Regulation of cell death: the calcium-apoptosis link. Nat. Rev. Mol. Cell Biol. *4*, 552–565.

Pacher, P., and Hajnoczky, G. (2001). Propagation of the apoptotic signal by mitochondrial waves. EMBO J. *20*, 4107–4121.

Petersen, O.H., Tepikin, A., and Park, M.K. (2001). The endoplasmic reticulum: one continuous or several separate Ca(2+) stores? Trends Neurosci. *24*, 271–276.

Pinton, P., Ferrari, D., Magalhaes, P., Schulze-Osthoff, K., Di Virgilio, F., Pozzan, T., and Rizzuto, R. (2000). Reduced loading of intracellular Ca(2+) stores and downregulation of capacitative Ca(2+) influx in Bcl-2-overexpressing cells. J. Cell Biol. *148*, 857–862.

Pinton, P., Ferrari, D., Rapizzi, E., Di Virgilio, F.D., Pozzan, T., and Rizzuto, R. (2001). The Ca2+ concentration of the endoplasmic reticulum is a key determinant of ceramide-induced apoptosis: significance for the molecular mechanism of Bcl-2 action. EMBO J. *20*, 2690–2701.

Rizzuto, R., Pinton, P., Carrington, W., Fay, F.S., Fogarty, K.E., Lifshitz, L.M., Tuft, R.A., and Pozzan, T. (1998). Close contacts with the endoplasmic reticulum as determinants of mitochondrial Ca2+ responses. Science *280*, 1763–1766.

Rizzuto, R., Pinton, P., Ferrari, D., Chami, M., Szabadkai, G., Magalhaes, P.J., Di Virgilio, F., and Pozzan, T. (2003). Calcium and apoptosis: facts and hypotheses. Oncogene *22*, 8619–8627.

Scorrano, L., and Korsmeyer, S.J. (2003). Mechanisms of cytochrome c release by proapoptotic BCL-2 family members. Biochem. Biophys. Res. Commun. *304*, 437–444.

Scorrano, L., Oakes, S.A., Opferman, J.T., Cheng, E.H., Sorcinelli, M.D., Pozzan, T., and Korsmeyer, S.J. (2003). BAX and BAK regulation of endoplasmic reticulum Ca2+: a control point for apoptosis. Science *300*, 135–139.

Smirnova, E., Shurland, D.L., Ryazantsev, S.N., and van der Bliek, A.M. (1998). A human dynamin-related protein controls the distribution of mitochondria. J. Cell Biol. *143*, 351–358.

Smirnova, E., Griparic, L., Shurland, D.L., and van der Bliek, A.M. (2001). Dynamin-related protein Drp1 is required for mitochondrial division in mammalian cells. Mol. Biol. Cell *12*, 2245–2256.

Szalai, G., Krishnamurthy, R., and Hajnoczky, G. (1999). Apoptosis driven by IP(3)-linked mitochondrial calcium signals. EMBO J. *18*, 6349–6361.

Wang, H.G., Millan, J.A., Cox, A.D., Der, C.J., Rapp, U.R., Beck, T., Zha, H., and Reed, J.C. (1995). R-Ras promotes apoptosis caused by growth factor deprivation via a Bcl-2 suppressible mechanism. J. Cell Biol. *129*, 1103–1114.

Yaffe, M.P. (1999). The machinery of mitochondrial inheritance and behavior. Science *283*, 1493–1497.

Yoon, Y., and McNiven, M.A. (2001). Mitochondrial division: new partners in membrane pinching. Curr. Biol. *11*, R67–R70.

Zong, W.X., Li, C., Hatzivassiliou, G., Lindsten, T., Yu, Q.C., Yuan, J., and Thompson, C.B. (2003). Bax and Bak can localize to the endoplasmic reticulum to initiate apoptosis. J. Cell Biol. *162*, 59–69.